Journal of Energy Chemistry 40 (2020) 180–187

Contents lists available at ScienceDirect

Journal of Energy Chemistry

journal homepage: www.elsevier.com/locate/jechem

http://www.journals.elsevier.com/journal-of-energy-chemistry/

Low-bandgap polymers with quinoid unit as Π bridge for high-performance solar cells

Bilal Shahid[a,b], Xiyue Yuan [a,b], Qian Wang [a], Di Zhou [a,b], Ergang Wang [c], Xichang Bao[a], Dangqiang Zhu[a,*], Renqiang Yang [a,*]

[a] Qingdao Institute of Bioenergy and Bioprocess Technology, Chinese Academy of Sciences, Qingdao 266101, Shandong, China
[b] Center of Materials Science and Optoelectronics Engineering, University of Chinese Academy of Sciences, Beijing 100049, China
[c] Department of Chemistry and Chemical Engineering/Applied Chemistry, Chalmers University of Technology, Gothenburg SE-412 96, Sweden

article info

Article history:
Received 17 February 2019
Revised 29 March 2019
Accepted 3 April 2019
Available online 13 April 2019

Keywords:
Low bandgap polymer
Side-chain engineering
Quinone structure
Π -bridging

abstract

To construct efficient low band gap polymers, increasing the Quinone structure of the polymer backbone could be one desirable strategy. In this work, two D–Q–A–Q polymers P1 and P2 were designed and synthesized with thiophenopyrrole diketone (TPD) and benzothiadiazole (BT) unit as the core and ester linked thieno[3,4-*b*]thiophene (TT) segment as Π -bridging, and the main focus is to make a comparative analysis of different cores in the influence of the optical, electrochemical, photochemical and morphological properties. Compared with the reported $PBDTT_{EH}$–$TBTT_{HD-i}$, P1 exhibited the decreased HOMO energy level of −5.38 eV and lower bandgap of 1.48 eV. Furthermore, when replaced with BT core, P2 showed a red-shifted absorption profile of polymer but with up-shifted HOMO energy level. When fabricated the photovoltaic devices in conventional structure, just as expected, the introduction of ester substituent made an obvious increase of V_{OC} from 0.63 to 0.74 V for P1. Besides, due to the deep HOMO energy level, higher hole mobility and excellent phase separation with $PC_{71}BM$, a superior photovoltaic performance (PCE = 7.13%) was obtained with a short-circuit current density (J_{SC}) of 14.9 mA/cm^2, significantly higher than that of P2 (PCE = 2.23%). Generally, this study highlights that the strategy of inserting quinoid moieties into D–A polymers could be optional in LBG-polymers design and presents the importance and comparison of potentially competent core groups.

1. Introduction

In recent past, organic photovoltaic (OPV) has become one of the most researched topics for the sources of energy which could be easily revitalized. The light weight, flexible and color adjustable OPV materials have become the beacon of hope for scientists and economists for affordable alternate source of energy [1,2]. The structure of bulk heterojunction (BHJ) solar cell devices normally consist of *p*-type conjugated polymers as electron-donors and *n*-type materials as electron-acceptors [3–6]. One of the key research directions for BHJ type of OSCs has been the design of low-band-gap polymers of E_g < 1.5 eV, which could be in favor of obtaining a broad absorption profile with as much as possible energy absorption to elevate the photocurrent. However, the major obligation in LBG polymers is to reach the level of adequate energy offset between HOMO and LUMO levels of the fullerene, and to exhibit the competency to turn excitons into free charges. Therefore, two basic strategies have been proven very effective in designing low band-gap polymers of stabilizing the quinoid (Q) resonance structure [7] and utilizing donor (D)-acceptor (A) interactions [8–10]. To realize the low bandgap of <1.5 eV, generally, strong acceptor (such as pyrrolo [3,4-*c*]pyrrole-1,4-dione (DPP), isoindigo, naphtho[1,2-*c*:5,6-*c*′]bis[1,2,5]thiadiazole (NTz)) or donor moiety (such as 2,2-bithiophene (2T), dithieno-[3,2-*b*:2,3-*d*]pyrrole (DTP)) could be used (Fig. S1), in which, the well-known DPP derivatives have been considerably most focused class as normally the optical band gap of copolymers conventionally have been under 1.5 eV with desirable efficiency of >7% [11–15]. However, it seems difficult to further optimize the electronic energy levels just through the single D–A strategy. Thus, it is essential to develop novel molecular strategy to construct efficient low band gap polymers [6,16].

As we all know, increasing the Quinone structure of the polymer backbone could be in favor of its capability to bring the polymer in class of narrow band gap [17]. For example, the thiophenopyrrole diketone (TPD) has wide bandgap of energy

* Corresponding authors.
E-mail addresses: zhudq@qibebt.ac.cn (D. Zhu), yangrq@qibebt.ac.cn (R. Yang).

https://doi.org/10.1016/j.jechem.2019.04.007

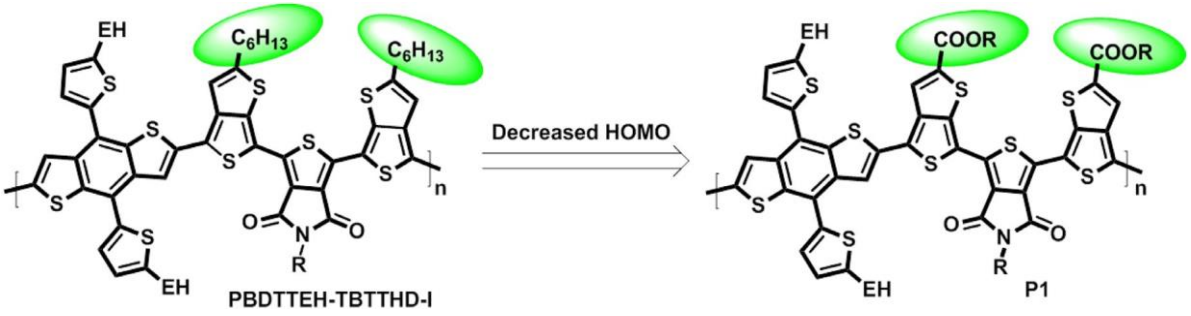

Fig. 1. New employed strategy of the modification in polymer structure.

normally (E_g^{opt} = 1.8 eV) with very mediocre competency in OSCs, for instance, when copolymerized with benzo[1,2- *b*:4,5-*b′*]dithiophene (BDT) [18,19]. However, the quinoid group thieno[3,4-*b*]thiophene (TT) as bridging component and respective impact can enhance or decrease the competency of polymers. The optical absorption of the polymer $PBDT_{TEH}$–$TBTT_{HD-i}$ was broadened to 726 nm with the band gap of approximately 1.5 eV, and the corresponding devices could give maximum efficiency of 6.47% in conventional structure (Fig. 1) [18]. However, the V_{OC} significantly decreased from the 1.00 to 0.64 V, which further restricted its development. The limitation of structural upgradation was similarly noted in benzothiadiazole (BT) based polymers [20–22]. Thus, further variation was needed to upgrade the performance and optimization of these types of structures and study their upgradation process.

Besides, the side chains have capability to alter the characteristic energy profiles of polymers by enhancing or diminishing various vital characteristics like tuning of solubility, thermal stability of BHJ OSCs, impacting the rate of crystallization and dimerization of fullerene, electron affinity, polymer packing, morphology, eventually device efficiency and others [19,23–28]. As compared to the electron-donating alkyl side chain, the electron-withdrawing ester linked side chain group is very impactful in lowering the HOMO energy level with increased crystallinity and exhibiting high density of π –π^* stacking. Meanwhile, the non-covalent interactions between O and S could also make the structure more compact and planar [29]. For example, Hou and co-workers synthesized polymers based on polythiophene derivatives with majorly introducing the ester linked side chain in structure which ultimately resulted in PCE of 7.2% with V_{OC} = 0.91 V, significantly superior to the photovoltaic performance based on P3HT (PCE of only 1.8% and V_{OC} = 0.63 V) [30].

In this study, two D–Q–A–Q polymers (P1 and P2) were designed and synthesized with TPD or BT unit as the core and ester linked TT segment as π-bridging, and the main focus is to make a comparative analysis of different cores in the influence of the optical, electrochemical, photochemical and morphological properties [31]. Compared with $PBDT_{TEH}$–$TBTT_{HD-i}$ [18], P1 exhibited the decreased HOMO energy level of −5.38 eV and lower bandgap of 1.48 eV. So, the impact of structural modification and side-engineering does have its good signs on the polymer potential. Furthermore, when replaced with BT core, P2 showed a red-shifted absorption profile of polymer but with up-shifted HOMO energy level and poor performance due to the lower hole mobility, and less favorable morphology. When fabricated the photovoltaic devices in conventional structure, just as expected, the introduction of ester substituent made an obvious increase of V_{OC} from 0.63 to 0.74 V for P1. Besides, due to the deep HOMO energy level, higher hole mobility and excellent phase separation with $PC_{71}BM$, a superior photovoltaic performance (PCE=7.13%) was obtained with a short-circuit current density (J_{SC}) of 14.9 mA/cm^2, significantly higher than that of P2 (PCE=2.23%). Generally, this study highlights that the strategy of inserting quinoid moieties into D–A polymers could be beneficial in LBG-polymers design and presents the importance and comparison of potentially competent core groups.

2. Experimental

2.1. Materials

All chemical reagents and materials were purchased from commercial sources and used without further purification, unless otherwise mentioned. Toluene (PhMe) and tetrahydrofuran (THF) were distilled over sodium in the presence of benzophenone as indicator. *N,N*-dimethylformamide (DMF) was distilled over calcium hydride. Compounds 1 and monomer 2D-BDT-Sn were synthesized according to the previous literatures [32,33].

2.2. Sample preparation

2.2.1. Compound 2

Compound 1 (1.7323 g, 2.7 mmol) and 1,3-dibromo-5-octyl-4H-thieno[3,4-*c*]pyrrole-4,6(5H)-dione (TPD, 0.3935 g, 0.9 mmol) were added to the double neck RBF and air was removed from the mixture. The catalyst tetra-triphenylpalladium (0.144 g) was added quickly to the flask under Argon protection. Then after the addition of toluene (25 mL), the mixture was refluxed at 110 ℃ for 24 h, and then the toluene was evaporated by vacuum distillation and rotary evaporator. Subsequently, the residue was extracted by adding water and DCM, and the organic phase was separated, dried by anhydrous sodium sulfate. Then, column chromatographically was done with PE and DCM (2:1) as eluent. The product obtained was orange solid (1.174 g, 68%). ^{1}H NMR (600 MHz, $CDCl_3$): δ (ppm): 7.85 (s, 2H), 7.72 (s, 2H), 4.27 (d, 4H), 3.69 (t, 2H), 1.83–1.80 (m, 2H), 1.72–1.69 (m, 2H), 1.43–1.28 (m, 42H), 0.92–0.84 (m, 15H)

2.2.2. Compound 3

Compound 2 (0.382 g, 0.389 mmol) was added into the RBF followed by trichloromethane (50 mL). Then, *N*-bromosuccinimide (NBS, 0.152 g, 0.85 mmol) was added in parts. At room temperature, the reaction mixture was stirred for 4 h and the washing with sodium thiosulfate solution was done. Later the solvent extraction with DCM and drying with anhydrous sodium sulfate gave organic phase, which was concentrated and then subjected to purification process by neutral alumina column chromatography with PE and DCM (4:1) as eluent. The product was precipitated in methanol, filtered and then dried in vacuum oven which gave eventually reddish brown solid (0.069 g, 20%). ^{1}H NMR (600 MHz, $CDCl_3$): δ (ppm): 7.61 (s, 2H), 4.29 (d, 4H), 3.68 (t, 2H), 1.84–1.80 (m, 2H), 1.72–1.68 (m, 2H), 1.43–1.25 (m, 42H), 0.92–0.84 (m, 15H).

2.2.3. Compound 4

Compound 1 (1.7323 g, 2.7 mmol) and 4,7-dibromobenzo[1,2,5]thiadiazole (BT, 0.264 g, 0.9 mmol) were

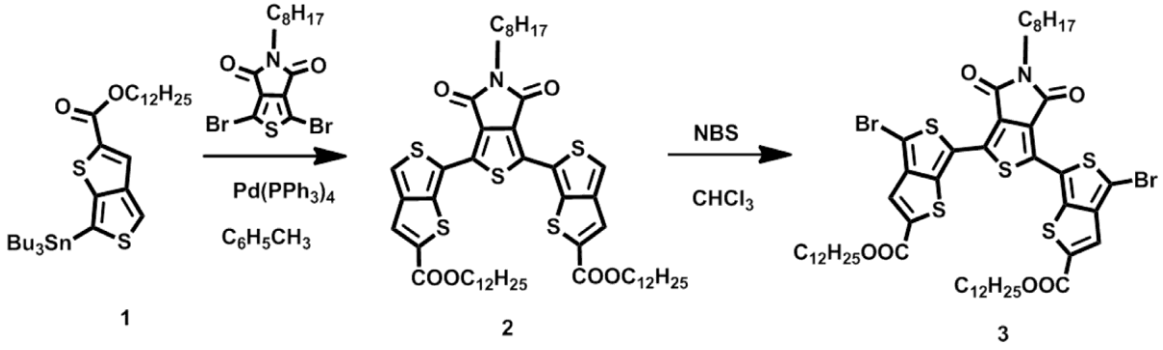

Scheme 1. Synthetic route of TPD monomer.

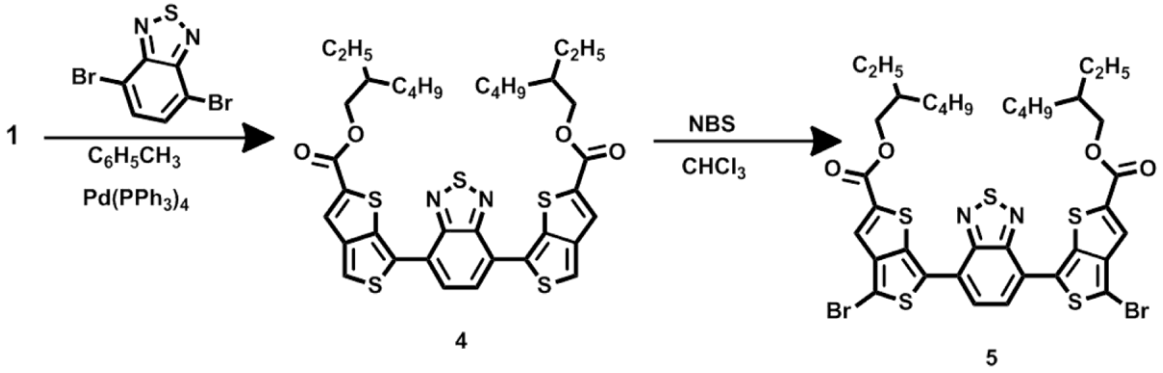

Scheme 2. Synthetic route of BT monomer.

reacted with similar procedure as synthesis of 3 with the catalyst tetra-triphenylpalladium (0.144 g) under Argon protection and toluene (25 mL) as solvent. After refluxing the mixture at 110 ℃, the washing was done. Later the column chromatographically was done with PE and DCM (2:1) as eluent. The product obtained was black (0.42 g, 65%). ^{1}H NMR (600 MHz, $CDCl_3$): δ (ppm): 7.89 (s, 2H), 7.81 (s, 2H), 7.71 (s, 2H), 4.31–4.28 (m, 4H), 1.79–1.75 (m, 2H), 1.54–1.38 (m, 16H), 1.06–0.92 (m, 12H).

2.2.4. Compound 5

Compound 4 (0.42 g, 0.58 mmol) was added into the RBF followed by trichloromethane (50 mL) and then, *N*-bromosuccinimide (NBS, 0.225 g, 1.26 mmol) was added in parts. At room temperature, the reaction mixture was stirred for 4 h and the washing with sodium thiosulfate solution was done. Later the solvent extraction with DCM and drying with anhydrous sodium sulfate gave organic phase, which was concentrated and then subjected to purification process by neutral alumina column chromatography with PE and DCM (4:1) as eluent. The product was precipitated in methanol, filtered and then dried in vacuum oven, which gave finally black solid (0.35 g, 70%). ^{1}H NMR (600 MHz, $CDCl_3$): δ (ppm): 7.78 (s, 2H), 7.61 (s, 2H), 4.31–4.29 (t, 4H), 1.81–1.77 (m, 2H), 1.52–1.39 (m, 16H), 1.02–0.96 (m, 12H).

2.2.5. Synthesis of polymers

2.2.5.1. General procedure of polymerization for P1 and P2. To a 25 mL round-bottom flask, compound 3 or compound 5 (0.2 mmol), bis(trimethyltin)benzothiophene (BDT, 0.2 mmol) and toluene (5 mL) were added. Later, the mixture was purged with argon for 20 min followed by adding the catalyst $Pd(PPh_3)_4$ (0.01 mmol, 11.5 mg). And then after being purged with argon for another 40 min, the mixture was heated at 110 ℃ for 12 h. After cooling to room temperature, the mixture was dropped in methanol. After the filtration, the precipitate was packed in filter paper, subjected to Soxhlet extraction, and then the product was precipitated with methanol. Later, the product was filtered and dried overnight under vacuum at 40 ℃. P1 was reddish brown solid film with metallic luster and P2 was dark blue color solid.

3. Results and discussion

The synthetic route of the monomers were shown in Schemes 1 and 2 and the details are described in Experimental section [9].

3.1. Physical characteristics of polymers

Two polymers P1 and P2 were prepared through Stille coupling reaction with a mixed solvent of toluene/DMF (Scheme 3). P1 and P2 were reasonably well soluble in common solvent, such as chlorobenzene (CB) and o-dichlorobenzene (o-DCB), which could be favorable for solution processing in device fabrication. The thermal stability of polymers was analyzed by using thermogravimetric analysis (TGA), as shown in Fig. S1. P1 polymer exhibited better thermal stability quality by showcasing onset decomposition temperatures (T_d) corresponding to 5% weight loss at 366 ℃ while P2 polymer only displayed T_d at 236 ℃. So, P1 has more potential to successfully perform in OSCs at high temperature with superior thermal strength.

3.2. Computational study of polymers

The computational study of both polymers for the calculation of energies and distributions of the frontier molecular orbitals was executed by density functional theory (DFT) using the Gaussian 09 program at the B3LYP/6-31G(d,p) level. For the simplification of calculation and shorter time duration, one repeating unit of methyl group was used instead of alkyl groups. The HOMO and LUMO energy levels of the polymers P1 and P2 are presented with minimized conformational structures as well in Fig. 2. The dihedral angles between TT moiety and TPD are 0.1734° and 0.0252°

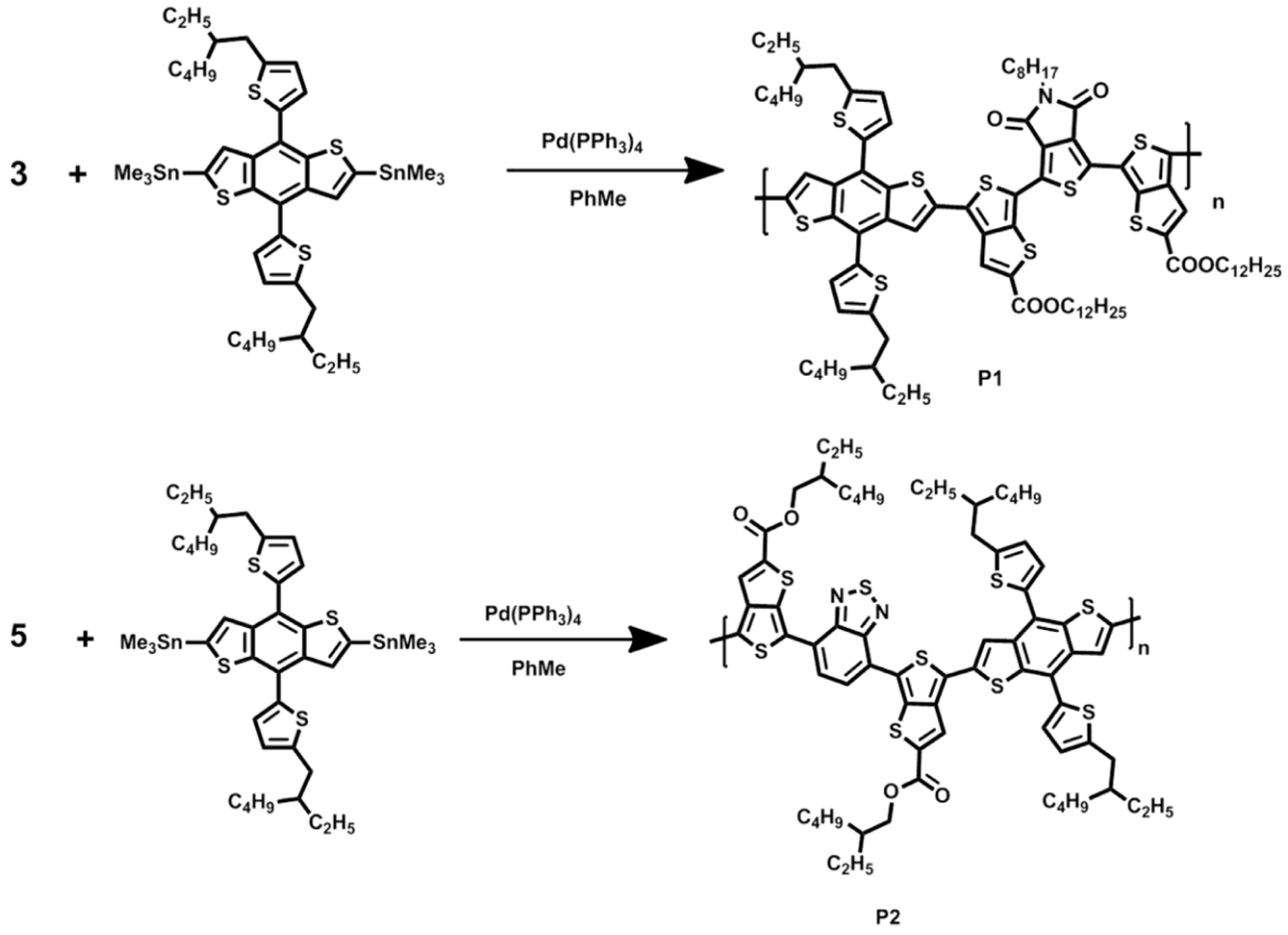

Scheme 3. Synthetic route of polymers P1 and P2.

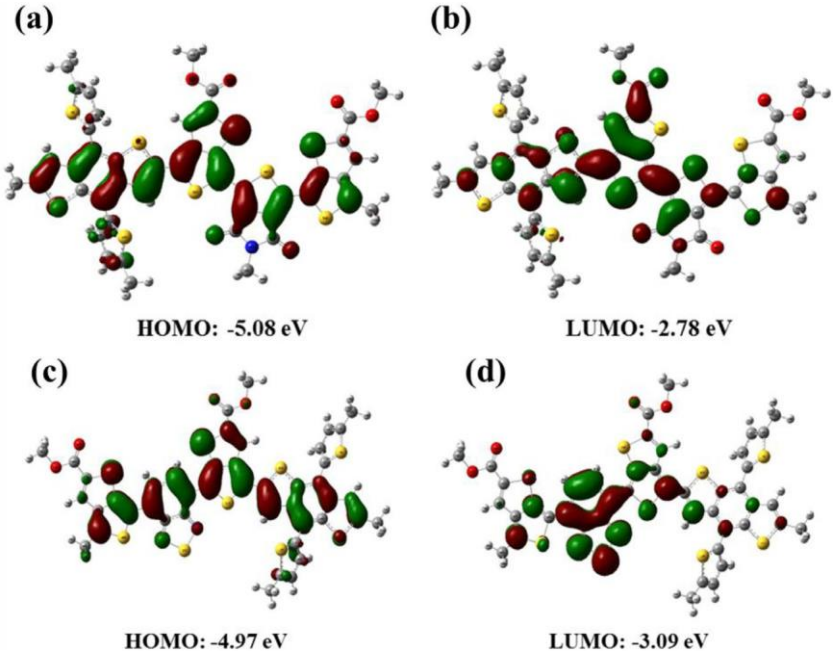

Fig. 2. (a) HOMO and (b) LUMO energy levels of P1 and (c) HOMO and (d) LUMO energy levels of P2. Colour description: Grey (Carbon); White (Hydrogen); Blue (Nitrogen); Yellow (Sulfur); Red (Oxygen).

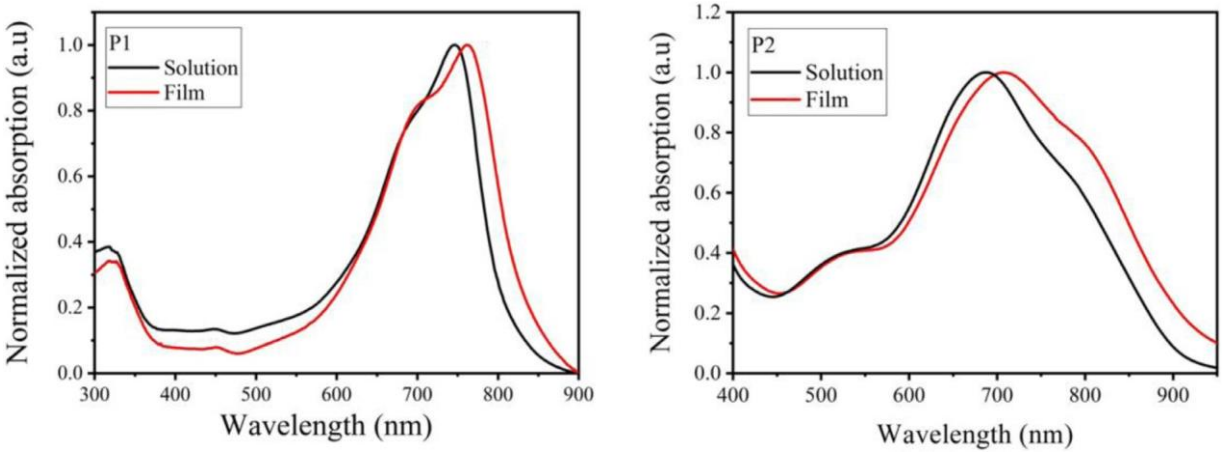

Fig. 3. UV absorption spectra of polymer P1 and P2 in solution and film state.

Table 1. Optical and electrochemical properties of P1 and P2.

Polymer	Solution λ_{max} (nm)	Film λ_{max} (nm)	Film λ_{onset} (nm)	E_g^{opt} (eV)	HOMO (eV)
P1	743	762	836	1.48	−5.38
P2	690	707	935	1.32	−5.07

whereas the angle between BT and TT are 1.13 ° and 1.57 °. These small angles implicate that both polymers have good planar structural arrangement. The very small dihedral angles between TT and core units could be ascribed to the non-covalent interactions between sulfur in adjacent TT and accepting units [34–36]. In Fig. 2, the HOMO energy levels are distributed and delocalized on almost all the structure while LUMO is mainly constrained on the acceptor unit. Besides, the smaller HOMO-LUMO gap for P2 repeating unit suggests that P2 will possess the lower bandgap, but with a higher HOMO energy level. All these calculations assert the probable aptitude of this new structural framework which is showing better planarity and conformation than previous literature and also depicting a fair assessment between two potentially very competent accepting groups. In addition, P1 exhibited deeper HOMO energy level but P2 with lower optical bandgap.

3.3. Optical properties

The ultraviolet-visible (UV–vis) absorption spectra of the two polymers are presented in Fig. 3 with comprehensive data in Table 1. Both polymers P1 and P2 exhibit broad absorption spectrum in range of 600–900 nm. The maximum absorption peak of P1 and P2 is found at 743 and 690 nm for solution, 762 and 707 nm for film state, respectively. The onset wavelength values (λ_{onset}) of P1 and P2 in film state are 836 and 935 nm respectively and the bandgap obtained on the basis of these values was calculated to be 1.48 and 1.32 eV. The absorption peak value of P1 is higher than 725 nm of $PBDT_{TEH}$–$TBTT_{EH-i}$, which might be due to that the introduction of ester groups to TT units enhance the electron-withdrawing ability and then increase intramolecular charge transfer of P1. The absorption curves of P1 in solution state and film state show similar profile, moreover, the maximum peak of absorption from solution to film red-shift only 4 nm. These results corporately indicate the strong aggregation behavior for P1. In contrast, P2 demonstrates a significant red-shift than that of P1, which could be attributed to that the acceptor strength of BT is higher than TPD. The above results strongly confirmed that increasing the quinoid structure of the backbone could be favorable to give low bandgap poly mers.

3.4. Electrochemical properties

For the better and efficient PSCs, particularly the values of V_{OC} are very vital factor, which are directly related and majorly reliant on matching the energy levels of both donors and acceptors. Cyclic voltammetry (CV) was carried out for the electrochemical characteristic behaviors and HOMO and LUMO measurements of the both polymers. The standardization of saturated calomel reference electrode (SCE) was done employing the ($E_{1/2}^{(Fc/Fc+)}$) arrangement at 4.40 eV and the oxidation onset potential of the P1 and P2 was calculated to be at 0.98 and 0.67 V, respectively (Fig. 4). The formula $E_{HOMO} = -(E_{on}^{ox} + E_{\frac{1}{2}}^{(Fc/Fc^+)})$eV was employed for calculation of HOMO level which was 5.38 and −5.07 eV for P1 and P2 correspondingly, which was consistent with the calculations (Table 1). The value of HOMO level of both polymers P1 and P2 was relatively lower than those of the previously reported polymers which mean that both polymer films will be more suitable and appropriate for obtaining high values of V_{OC} after blending with PCBM than the previously reported similar polymer structures. The energy orbital values especially HOMO level are more deep and lower in P1 than P2 polymer. So, it can be anticipated that P1 is capable to attain higher V_{OC} in OSCs because V_{OC} is proportional to the offset between the HOMO of polymeric donor and the LUMO of the fullerene acceptor.

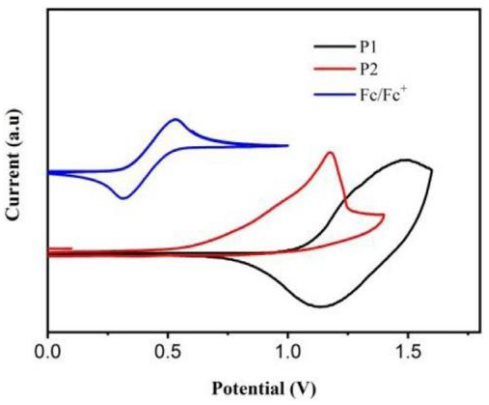

Fig. 4. Cyclic voltammogram curves of P1 and P2.

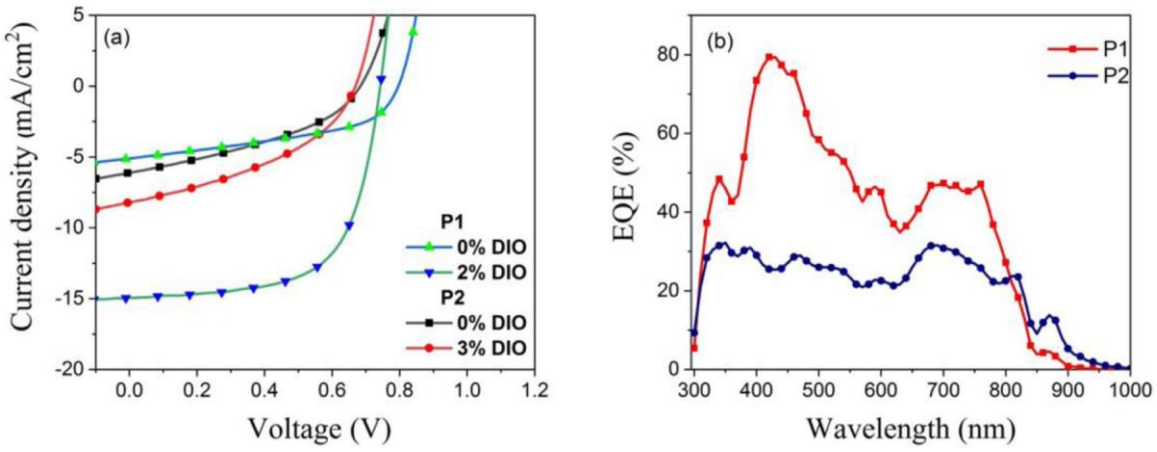

Fig. 5. (a) *J–V* curve and (b) EQE graph of the devices based P1 and P2.

Table 2. Photovoltaic performance parameters of polymers.

Polymer	Additive (DIO)	V_{OC} (V)	J_{SC} (mA/cm^2)	FF (%)	PCE (%)
P1	2%	0.74	14.9	64.3	7.13
$PBDT_{TEH}$–$TBTT_{HD-i}$[18]	0	0.63	15.93	64.76	6.47
P2	3%	0.66	8.20	40.8	2.23

3.5. Photovoltaic performance

For the photovoltaic characteristic study of polymers in solar cell, the fabrication of bulk heterojunction solar cells was done by using traditional device structures comprising of ITO/PEDOT:PSS/Polymer:$PC_{71}BM$/PFN-Br/Al. In the conventional device structure, the role of PEDOT:PSS is normally to assist the hole extraction, while, the role of hole blocking and electron extraction is attributed to PFN-Br. Other factors including solvent additive, D/A ratio also have vital role in performance of polymer solar cell. The detailed evaluation of competency of polymer P1 and P2 in OSC device structures under different working conditions has been depicted in Tables 2 and S2 and *J–V* curves are displayed in Figs. 4 and S2.

The device results without any DIO additive in both polymers were not very encouraging but with the addition of DIO, the performance started to improve in key factors of devices, more specifically, the J_{SC} and fill factor (FF). It could be attributed to the improvement of the morphology of active layer, which will be discussed later. The photovoltaic devices based polymer P1 with the TPD core unit showed a power conversion efficiency (PCE) of 7.13% with V_{OC} of 0.74 V, J_{SC} of 14.9 mA/cm^2, and FF of 64.3%, which is better than the reported analogues $PBDT_{TEH}$–$TBTT_{HD-i}$ (V_{OC} = 0.63 V and PCE = 6.47%). This result confirmed that our expectation of ester substituent could be favorable for V_{OC}. By contrast, the polymer P2 which contains BT only showed the V_{OC} of 0.66 V and J_{SC} of 8.20 mA/cm^2, leading to a poor efficiency of 2.23% [37]. Furthermore, the efficiency of 7.13% is clearly one of higher range values of LBG polymer based PSCs (Table S1). More importantly, this new D–Q–A–Q structural arrangement could give a prospective path to further upgrade for the LBG class of polymer through the choice of the core, device engineering. In-depth explanation of TPD unit exhibiting more potential to gain in similar structural arrangement than that of BT could be explained by the further analysis and studies like photoluminescence test (PL), charge-carrier mobility assessment and morphological investigation.

The external quantum efficiency (EQE) analysis was done for both polymers P1 and P2 by obtaining spectra under illumination of monochromatic light. From Fig. 5, the J_{SC} integrated from the EQE spectra of P1 and P2 is approximately similar with experimental J_{SC} values within the possibility of 10% error. The devices of both of the narrow band-gap polymers based on TPD and BT demonstrate broad range spectra between 300 and 850 nm. The relatively high photo-response for P1 could be one main reason to give higher value of J_{SC}. In addition, charge-carrier mobility assessment by the space charge limited current (SCLC) method gives the values of charge-carrier mobility which is key factor for the competency of OSC devices. The hole mobility of P1 and P2 was obtained by employing the device structure of ITO/PEDOT:PSS/Polymer:$PC_{71}BM$/Au. As shown in Fig. 6, the values obtained from technique depict that the hole mobilities (μ_h) of two devices comprising P1 and P2 are 5.56×10^{-4} cm^2 V^{-1} s^{-1} and 2.98×10^{-5} cm^2 V^{-1} s^{-1} respectively. High mobility could be favorable for effective charge carrier transport and reduce the photocurrent loss in photovoltaic devices. Thus, P1-based devices exhibited high J_{SC}, leading to the excellent performance.

3.6. Photoluminescence spectroscopy

The photoluminescence (PL) spectra of pure polymers and blend film were examined to investigate the exciton dissociation behaviors in the blends (Fig. S3). It is obvious that the excitons in blend film of P1:$PC_{71}BM$ showed effective dissociation. On the contrast, a large amount of excitons in P2:$PC_{71}BM$ could not separate into free charges successfully, indicating severe geminate recombination in this blend. It explains why devices based on P2 showed low current density compared with P1, although P2 has broader absorption.

3.7. Morphological characterization

The morphology of the active layer blend plays a vital role in the charge transport and charge separation. Transmission electron microscopy (TEM) is employed to investigate the morphology of polymers after modification in device with and without additive DIO (Fig. 7). In the case of P1, when no additive was added, the blend film showed strong phase separation which might be unfavorable of exciton transfer. With addition of DIO, the observable aggregations in P1:$PC_{71}BM$ blend film fade and fibrous interpenetrating network appears which is favorable for charge transport and separation and it also visibly affirms the influence of DIO on

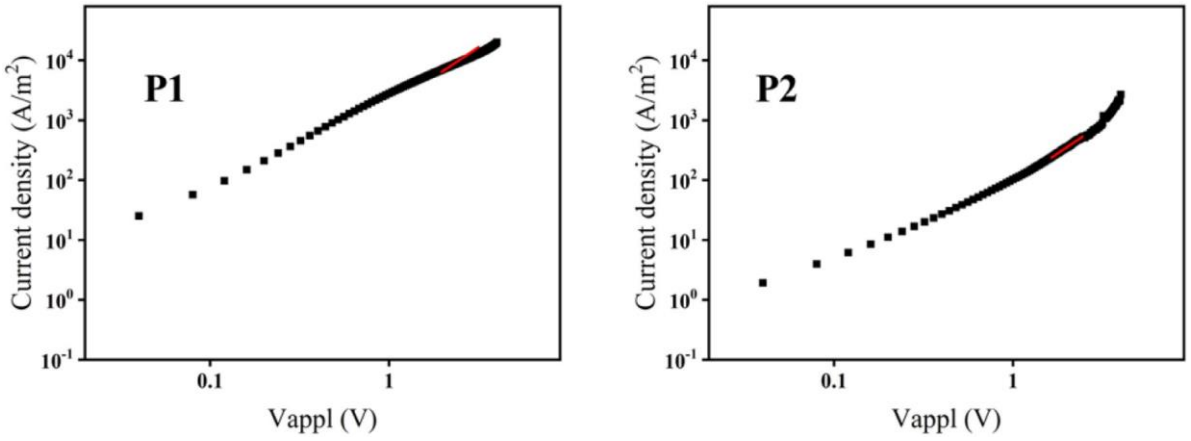

Fig. 6. Current density-voltage (*J*–*V*) curves of Polymer:$PC_{71}BM$.

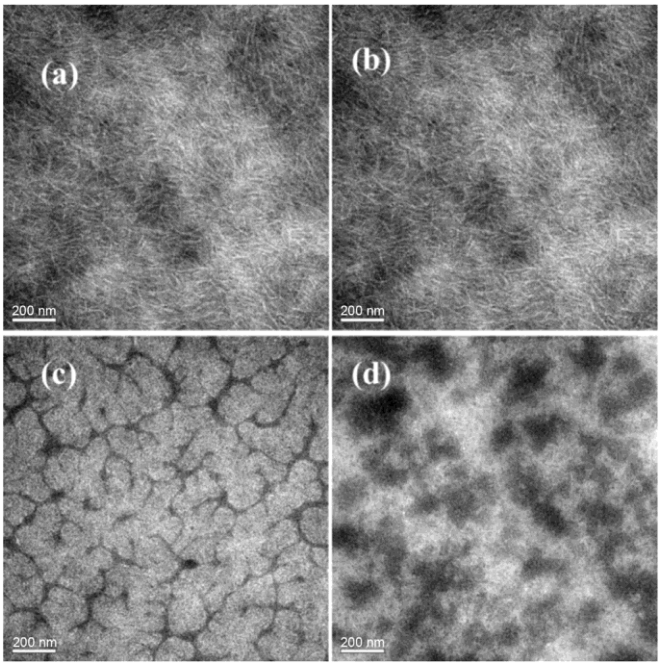

Fig. 7. TEM images of P1/$PC_{71}BM$ blend films (a) without and (b) with DIO and P2/$PC_{71}BM$ blend films (c) without and (d) with DIO. The scale bar is 200 nm.

phase separation exciton separation [31]. The addition of DIO decreases the aggregation in P2:$PC_{71}BM$ blend as well, which is very significantly detectable on the TEM images. However, the crystallinity in P2 based blend is still in micrometer size, which is much longer than the diffusion length of excitons. The difference between morphology of P2 based and P1 based blend film agrees well with the results obtained from PL spectra. The anticipated nanophase structural arrangement usually tends to favor escalation of J_{SC} and FF in the blend films which is dually proved in P1 with improved high values of both features whereas in P2 such behavior is not showcased.

4. Conclusions

In summary, to develop the efficient LBG polymer, two polymers P1 and P2 based the new D–Q–A–Q arrangement were synthesized with different core groups like TPD and BT and a comparative study was executed to investigate the potential of core groups. The P1 polymers seemed to have adopted the new altered structure in a better effective manner than P2 because the comprehensive characteristic details of polymer visibly exhibit the improvement in all profiles of P1. The introduction of ester substituent makes the polymer P1 with decreased HOMO level of −5.38 eV but with a low bandgap of 1.48 eV. By contrast, the BT-based polymer P2 exhibited smaller E_g of 1.32 eV, but it could not give excellent performance due to the lower hole mobility, lower charge density and less favorable morphology. As a result, the TPD core unit based P1 showed a remarkable capability to gain from the similarly modified structural framework and improved greatly its photoelectric profile by attaining a high V_{OC} 0.74 V, J_{SC} 14.9 mA/cm^2, FF 64.3% and 7.13% efficiency, which is much greater than BT based polymer (2.23%) and almost 30% increased than the similar TPD based polymer (6.47%) from literature. It is established in this scenario that the TPD core unit is potentially more talented in comparison to BT for enhancing its properties. Overall, this work highlights the strategy of inserting quinoid moieties into D–A polymers, which could be beneficial in LBG-polymers design and presents the importance and comparison of potentially competent core groups.

Acknowledgments

The authors are deeply grateful to the National Natural Science Foundation of China (21604092, 51573205 and 51773220), China Postdoctoral Science Foundation (2017M610453), and the Youth Innovation Promotion Association CAS (2016194) for financial support. Bilal thanks the CAS-TWAS President's Fellowship Program for Ph.D.

Supplementary materials

Supplementary material associated with this article can be found, in the online version, at doi:10.1016/j.jechem.2019.04.007.

References

[1] C.J. Brabec, Solar Energy Mater. Solar Cells 83 (2004) 273–292.
[2] P.-L.T. Boudreault, A. Najari, M. Leclerc, Chem. Mater. 23 (2010) 456–469.
[3] H.-L. Yip, A.K.-Y. Jen, Energy Environ. Sci. 5 (2012) 5994–6011.
[4] J. Zhao, Y. Li, G. Yang, K. Jiang, H. Lin, H. Ade, W. Ma, H. Yan, Nat. Energy 1 (2016) 15027.
[5] H. Bin, L. Gao, Z.-G. Zhang, Y. Yang, Y. Zhang, C. Zhang, S. Chen, L. Xue, C. Yang, M. Xiao, Nat. Commun. 7 (2016) 13651.
[6] Y. Liang, Z. Xu, J. Xia, S.T. Tsai, Y. Wu, G. Li, C. Ray, L. Yu, Adv. Mater. 22 (2010) 135–138.
[7] J. Hou, H.-Y. Chen, S. Zhang, R.I. Chen, Y. Yang, Y. Wu, G. Li, J. Am. Chem. Soc. 131 (2009) 15586–15587.
[8] S. Li, L. Ye, W. Zhao, S. Zhang, S. Mukherjee, H. Ade, J. Hou, Adv. Mater. 28 (2016) 9423–9429.

[9] P. Sonar, E.L. Williams, S.P. Singh, A. Dodabalapur, J. Mater. Chem. 21 (2011) 10532–10541.
[10] J.H. Kim, S. Wood, J.B. Park, J. Wade, M. Song, S.C. Yoon, I.H. Jung, J.S. Kim, D.H. Hwang, Adv. Funct. Mater 26 (2016) 1517–1525.
[11] J.D. Chen, C. Cui, Y.Q. Li, L. Zhou, Q.D. Ou, C. Li, Y. Li, J.X. Tang, Adv. Mater. 27 (2015) 1035–1041.
[12] S.-H. Liao, H.-J. Jhuo, P.-N. Yeh, Y.-S. Cheng, Y.-L. Li, Y.-H. Lee, S. Sharma, S.-A. Chen, Sci. Rep. 4 (2014) 6813.
[13] M.C. Scharber, D. Mühlbacher, M. Koppe, P. Denk, C. Waldauf, A.J. Heeger, C.J. Brabec, Adv. Mater. 18 (2006) 789–794.
[14] W. Li, K.H. Hendriks, M.M. Wienk, R.A. Janssen, Acc. Chem. Res. 49 (2015) 78–85.
[15] R. Mondal, H.A. Becerril, E. Verploegen, D. Kim, J.E. Norton, S. Ko, N. Miyaki, S. Lee, M.F. Toney, J.-L. Brédas, J. Mater. Chem. 20 (2010) 5823–5834.
[16] H.-Y. Chen, J. Hou, S. Zhang, Y. Liang, G. Yang, Y. Yang, L. Yu, Y. Wu, G. Li, Nat. Photon. 3 (2009) 649.
[17] Y. Liang, L. Yu, Acc. Chem. Res. 43 (2010) 1227–1236.
[18] C. Zhang, H. Li, J. Wang, Y. Zhang, Y. Qiao, D. Huang, C.-a. Di, X. Zhan, X. Zhu, D. Zhu, J. Mater. Chem. A 3 (2015) 11194–11198.
[19] S.C. Price, A.C. Stuart, L. Yang, H. Zhou, W. You, J. Am. Chem. Soc. 133 (2011) 4625–4631.
[20] J. Hou, H.-Y. Chen, S. Zhang, G. Li, Y. Yang, J. Am. Chem. Soc. 130 (2008) 16144–16145.
[21] L. Dou, C.-C. Chen, K. Yoshimura, K. Ohya, W.-H. Chang, J. Gao, Y. Liu, E. Richard, Y. Yang, Macromolecules 46 (2013) 3384–3390.
[22] A.C. Stuart, J.R. Tumbleston, H. Zhou, W. Li, S. Liu, H. Ade, W. You, J. Am. Chem. Soc. 135 (2013) 1806–1815.
[23] C. Cui, W.Y. Wong, Macromol. Rapid Commun. 37 (2016) 287–302.
[24] Z. Li, F. Wu, H. Lv, D. Yang, Z. Chen, X. Zhao, X. Yang, Adv. Mater. 27 (2015) 6999–7003.
[25] D. Liu, Y. Zhang, G. Li, J. Energy Chem. 35 (2019) 104–123.
[26] J.M. Szarko, J. Guo, Y. Liang, B. Lee, B.S. Rolczynski, J. Strzalka, T. Xu, S. Loser, T.J. Marks, L. Yu, L.X. Chen, Adv. Mater. 22 (2010) 5468–5472.
[27] D.W. Chang, S.J. Ko, G.H. Kim, S.Y. Bae, J.Y. Kim, L. Dai, J.B. Baek, J. Polym. Sci. Part A Polym. Chem. 50 (2012) 271–279.
[28] Y. Guo, G. Han, Y. Yi, J. Energy Chem. 35 (2019) 138–143.
[29] M. Zhang, X. Guo, Y. Yang, J. Zhang, Z.-G. Zhang, Y. Li, Polym. Chem. 2 (2011) 2900–2906.
[30] M. Zhang, X. Guo, W. Ma, H. Ade, J. Hou, Adv. Mater. 26 (2014) 5880–5885.
[31] J.C. Bijleveld, V.S. Gevaerts, D. Di Nuzzo, M. Turbiez, S.G. Mathijssen, D.M. de Leeuw, M.M. Wienk, R.A. Janssen, Adv. Mater. 22 (2010) 242–246.
[32] P. Liu, K. Zhang, F. Liu, Y. Jin, S. Liu, T.P. Russell, H.-L. Yip, F. Huang, Y. Cao, Chem. Mater. 26 (2014) 3009–3017.
[33] C. Zhang, Y. Zang, E. Gann, C.R. McNeill, X. Zhu, C.-a. Di, D. Zhu, J. Am. Chem. Soc. 136 (2014) 16176–16184.
[34] B. Sun, W. Hong, Z. Yan, H. Aziz, Y. Li, Adv. Mater. 26 (2014) 2636–2642.
[35] S. Shi, Q. Liao, Y. Tang, H. Guo, X. Zhou, Y. Wang, T. Yang, Y. Liang, X. Cheng, F. Liu, Adv. Mater. 28 (2016) 9969–9977.
[36] D. Liu, Q. Zhu, C. Gu, J. Wang, M. Qiu, W. Chen, X. Bao, M. Sun, R. Yang, Adv. Mater. 28 (2016) 8490–8498.
[37] H. Kim, H. Lee, Y. Jeong, J.-U. Park, D. Seo, H. Heo, D. Lee, Y. Ahn, Y. Lee, Syn. Metals 211 (2016) 75–83.